

Generalized moment expansion of dynamic correlation functions in finite Ising systems

Hans-Ulrich Bauer, Klaus Schulten, and Walter Nadler*

Physik-Department, Technische Universität München, James-Frank-Strasse, D-8046 Garching, Federal Republic of Germany

(Received 5 November 1987)

In this paper we study dynamic correlation functions of one- and two-dimensional kinetic Ising models, in particular, in situations where nonergodic behavior and critical slowing down emerge. We also investigate in how far nonexponential relaxation as described by a Williams-Watts function $\exp[-(t/\tau)^\beta]$ results in such systems. The method we apply is an expansion which simultaneously takes the high- and low-frequency behavior of observables into account (generalized moment expansion). This approximation can be applied to kinetic Ising models with arbitrary transition rate constants. Its computational effort does not increase when relaxation times diverge. However, the method involves the inversion of the transition operator and, hence, can be applied only to finite systems, the size of which depends on computational resources. We introduce a coarse graining of the state space which allows to extend the system size further and yields accurate magnetization correlation functions.

I. INTRODUCTION

Since their introduction by Lenz and Ising in 1925, Ising models have attracted much interest in connection with macroscopic equilibrium phenomena, in particular those involving cooperative effects. The models helped to explain ferromagnetic and antiferromagnetic behavior and the respective phase transitions. The history of the model has been presented by Brush.¹ Even though the formulation of the model is simple, exact analytic results can be obtained in a few cases only. Outstanding is the derivation of the partition function for the two-dimensional square lattice by Onsager.²

In 1963, Glauber triggered interest in the dynamics of the Ising model. In a pioneering study³ he carried out calculations on time-dependent observables of a (one-dimensional) Ising model with Markovian dynamics. Glauber considered, however, only simple rates governing the transitions between spin configurations in the field-free case, a constraint which allowed him to derive an exact analytical result. Later calculations have taken more complicated transition rates as well as external fields into account.⁴⁻⁶ The different approaches and results have been reviewed by Lacombe.⁷ Recent studies also investigated the critical dynamical exponent z , which, close to the critical point, links relaxation time (a nonequilibrium property) and correlation length (an equilibrium property). Depending on the choice of transition rates, z was found to assume values $z=2$ (Ref. 8), $z=4$ (Refs. 9 and 10), z in the range 2 to 4 (Ref. 11), $z=5$ (Ref. 12), and z in the range 2 to 5 (Ref. 13).

An important application of the dynamic Ising model is connected with polymers and their cooperative dynamics. The one-dimensional model can describe the kinetics of helix-coil transitions,^{14,15} if one interprets the spin state "up" as conformation state "helix," and the spin state "down" as conformation state "coil" of the polymer segments. Another interpretation considers the rotation of side groups of a chain molecule around the molecular

backbone. One associates with each side group a nonisotropic physical property which assumes a certain orientation relative to the backbone. There may be only two distinct orientations which can then be represented by a spin- $\frac{1}{2}$ model. A property of this kind is the electrical dipole moment of polar side groups¹⁶⁻¹⁹ and, hence, one expects an analogy between dielectric relaxation of a polymer and dynamic correlation functions of an Ising model.²⁰ In this respect it is of interest that the dielectric relaxation function $A(t)$ measured by photon-correlation spectroscopy can be described well by a Williams-Watts function²¹⁻²³

$$A(t) = \exp \left[- \left[\frac{t}{\tau} \right]^\beta \right]. \quad (1.1)$$

Several authors sought an explanation of this nonexponential behavior.^{19,24,25} Skinner explained this behavior by evoking the mentioned analogy with the Glauber model.^{26,27}

In previous investigations of the Glauber model, with the exception of Monte Carlo studies, the mathematical methods applied often dictated a particular choice of transition rates. Glauber himself, for example, chose one particular type of transition rate ("... motivated more by the desire for simplicity than for generality.") which up to now is the only type allowing an analytic description. In this paper we are interested in calculations of dynamic correlation functions for one- and two-dimensional Glauber models free of any restrictions with regard to a choice of transition rates. We will demonstrate that such calculations can be achieved by the generalized moment expansion (GME).²⁸⁻³⁴ However, this method is limited to finite systems. The method allows us, in particular, to study Williams-Watts behavior of correlation functions of the dynamic Ising model. We will investigate also nonergodicity and critical behavior of the kinetic Ising model which emerge in certain limits of the transition rates.

The limitation of the generalized moment expansion to

finite systems arises from the requirement of a numerical inversion of a matrix which describes the transitions between all spin configurations of the system investigated. The dimension d of this matrix has to be kept below some limit (for calculations on a conventional minicomputer, e.g., a Digital Equipment Corporation MicroVAX computer, $d \leq 2^{16}$, corresponding to 16 spins). In order to describe the magnetization correlation in systems with more spins we will introduce an effective rate approximation. This approximation allows us to investigate 25 spins in the two-dimensional case and over 100 spins in the one-dimensional case.

An alternative numerical method has been applied in Ref. 13 to finite dynamic Ising models with arbitrary transition rates. The method casts the corresponding master equation into Hamiltonian form and seeks the lowest nonvanishing eigenvalue λ_1 of the Hamiltonian by the Lanczos method. This eigenvalue appears in the spectral expansion of the correlation functions $C(t) = \sum_n \beta_n \exp(-\lambda_n t)$ and is interpreted as the longest relaxation time of $C(t)$. However, this interpretation holds only if β_1 is sufficiently large compared to the other β_n , and if the eigenvalues λ_n are sufficiently separated. If the relaxation of $C(t)$ involves two, three, ... very different time scales $\tau_1, \tau_2, \tau_3, \dots$ due to a clustering³⁵ of λ_n around values $\tau_1^{-1}, \tau_2^{-1}, \tau_3^{-1}, \dots$ the behavior of $C(t)$ is not properly described. The GME, in contrast, is well suited to reproduce the spectral expansion for rather arbitrary distribution of β_n and λ_n values.

The results obtained on finite systems by means of the GME, in principle, can be extrapolated to critical behavior of macroscopic systems by finite-size scaling (Ref. 36 provides a review of the latter). In this paper we do not consider such extrapolations since our issue is a demonstration of the GME for arbitrary high-dimensional master equations. Also our main example for the application of the GME below is the one-dimensional dynamic Ising model which exhibits a particular critical behavior and, therefore, may be a poor example for finite-size scaling. Furthermore, finite-size scaling applies only in the limit of large systems, and it is not clear if systems as small as investigated, for example, in Sec. V can be considered in the realm of finite-size-scaling theory.

II. ONE-DIMENSIONAL KINETIC ISING MODEL

We consider N spins σ_i with energy

$$H = -J \sum_{i=1}^N \sigma_i \sigma_{i+1}. \quad (2.1)$$

J denotes the coupling constant. An external magnetic field h could be taken into account by adding $h \sum_{i=1}^N \sigma_i$ to (2.1). We assume periodic boundary condition, i.e., $\sigma_0 \equiv \sigma_N, \sigma_1 \equiv \sigma_{N+1}$. Even though a spin interacts directly only with its two neighbors the static correlation length ξ grows beyond $\xi=1$ (in units of the lattice constant). In the infinite system the correlation length is related to the coupling strength J/kT by²⁶

$$\xi = \frac{1}{\ln[\coth(J/kT)]}. \quad (2.2)$$

The interpretation of this expression as a correlation length does not hold strictly in finite systems. The appropriate definition of a correlation length ξ_N for systems of size N and its relationship to ξ have been reviewed in Ref. 36.

For the dynamic properties of the model one requires: (i) only one spin reorients at a time (single-spin-flip model), (ii) the probability to reorient a spin depends symmetrically on the neighboring spins, (iii) the probability for spin flip remains invariant under inversion of all spins, (iv) the principle of detailed balance holds.

The most general rates w for transitions $\sigma_i \rightarrow -\sigma_i$ which comply with these requirements are³

$$w = \frac{\alpha}{2} \left[1 + \delta \sigma_{i-1} \sigma_{i+1} - \frac{\gamma}{2} (1 + \delta) \sigma_i (\sigma_{i-1} + \sigma_{i+1}) \right]. \quad (2.3)$$

The transition rates can assume only three values, w_{par} , w_{antipar} , and w_{mix} . These values and the spin configurations connected with them are

$$w_{\text{par}} = \frac{\alpha}{2} (1 + \delta)(1 - \gamma) \quad \begin{aligned} &\hat{=} \left\{ \begin{array}{l} \cdots \uparrow \uparrow \uparrow \cdots \rightarrow \cdots \uparrow \downarrow \uparrow \cdots \\ \cdots \downarrow \downarrow \downarrow \cdots \rightarrow \cdots \downarrow \uparrow \downarrow \cdots \end{array} \right\}, \end{aligned} \quad (2.4)$$

$$w_{\text{antipar}} = \frac{\alpha}{2} (1 + \delta)(1 + \gamma) \quad \begin{aligned} &\hat{=} \left\{ \begin{array}{l} \cdots \uparrow \downarrow \uparrow \cdots \rightarrow \cdots \uparrow \uparrow \uparrow \cdots \\ \cdots \downarrow \uparrow \downarrow \cdots \rightarrow \cdots \downarrow \downarrow \downarrow \cdots \end{array} \right\}, \end{aligned} \quad (2.5)$$

$$w_{\text{mix}} = \frac{\alpha}{2} (1 - \delta) \quad \begin{aligned} &\hat{=} \left\{ \begin{array}{l} \cdots \uparrow \uparrow \downarrow \cdots \leftrightarrow \cdots \uparrow \downarrow \downarrow \cdots \\ \cdots \downarrow \downarrow \uparrow \cdots \leftrightarrow \cdots \downarrow \uparrow \uparrow \cdots \end{array} \right\}. \end{aligned} \quad (2.6)$$

The parameters α, γ, δ specify the dynamics. α controls the time scale of the dynamics. γ is a measure of the coupling strength,

$$\gamma = \tanh(2J/kT), \quad -1 \leq \gamma \leq 1. \quad (2.7)$$

δ , to be interpreted below, can be expressed as

$$\delta = \frac{w_{\text{par}} - w_{\text{mix}}(1 - \gamma)}{w_{\text{par}} + w_{\text{mix}}(1 - \gamma)} \quad (2.8)$$

and, for the rates to remain positive, must be chosen in the range

$$-1 \leq \delta \leq 1. \quad (2.9)$$

At the boundaries of the allowed δ interval (2.9) some of the transition rates disappear. For example, for $\delta = +1$ holds

$$w_{\text{mix}} |_{\delta=1} = 0. \quad (2.10)$$

In this limit Bloch domains can be generated and annihilated, but Bloch walls, which separate clusters of up spins and clusters of down spins, are prohibited to migrate

along the chain by single steps. Bloch walls can move only in steps of two lattice spacings through a double-flip process

$$\cdots \uparrow \uparrow \downarrow \cdots \leftrightarrow \cdots \uparrow \downarrow \downarrow \cdots \leftrightarrow \cdots \uparrow \downarrow \downarrow \cdots \quad (2.11)$$

For $\delta = -1$ holds

$$w_{\text{par}} |_{\delta=-1} = w_{\text{antipar}} |_{\delta=-1} = 0. \quad (2.12)$$

In this limit the only allowed process is Bloch wall migration. Creation and annihilation of Bloch domains are prohibited and, hence, energy is conserved. For $\delta = 0$ cluster creation and migration are equally probable, since the sum of rates of forward and reverse transitions are equal for creation and migration. We collect the rates for different δ values in Table I.

Glauber actually proposed dynamics with general δ values, but he solely examined the case of vanishing δ . The Glauber solution for the spin autocorrelation function in an infinite ring is [η as in (A4)]

$$C_{\infty}(t) \equiv \langle \sigma_i(t) \sigma_i(0) \rangle |_{N=\infty} = e^{-\alpha t} \sum_{l=-\infty}^{\infty} I_l(\gamma \alpha t) \eta^{|l|}. \quad (2.13)$$

This result can be generalized to finite rings (see the Appendix):

$$C_N(t) \equiv \langle \sigma_i(t) \sigma_i(0) \rangle = e^{-\alpha t} \sum_{l=1}^N \sum_{j=-\infty}^{\infty} I_{i-l+jN}(\gamma \alpha t) \times \frac{\eta^{|l-i|} + \eta^{N-|l-i|}}{1 + \eta^N}. \quad (2.14)$$

Our algorithm presented below can be applied only to finite-spin systems. A comparison of the expressions (2.13) and (2.14) allows us to estimate how large a finite system must be in order that its relaxation behavior does not deviate from that of an infinite system. We found that for $N > 6\xi$ the correlation function $C_N(t)$ differs from C_{∞} by less than 1%. Since our computational resources (MicroVAX II) allow us to treat up to 16 spins (100 spins by means of the approximation of Sec. V) we expect that our results agree with those for an infinite system up to a coupling constant $J = 0.5$ kT. For higher J values size effects may become dominant in our results.

TABLE I. Transition rates w_{par} , w_{antipar} , and w_{mix} for different values of δ .

δ	w_{par}	w_{antipar}	w_{mix}
0	$\frac{\alpha}{2}(1-\gamma)$	$\frac{\alpha}{2}(1+\gamma)$	$\frac{\alpha}{2}$
-1	0	0	α
+1	$\alpha(1-\gamma)$	$\alpha(1+\gamma)$	0

III. GENERALIZED MOMENT EXPANSION

The generalized moment expansion (GME) is an approximation scheme which can reproduce the long-time as well as the short-time behavior of dynamical observables in stochastic systems.²⁹ It has been applied to lateral diffusion in membranes,³⁰ to Mössbauer absorption of Brownian particles,³¹ to equilibrium correlation functions in nonreactive Brownian processes,³² dynamic correlation functions in stochastic systems near instabilities,³³ and to observables connected with diffusion in dimension $d > 1$.³⁴ We present the GME in matrix notation, suitable for the discrete-state space of a spin system.

Let the state of the system at time t be characterized by a vector $\mathbf{p}(t)$, the i th component of which gives the probability of observing the system in state i . The state is assumed to be normalized, i.e., $\sum_i p_i(t) = 1$. The time evolution is governed by the master equation

$$\partial_t \mathbf{p}(t) = \mathbf{L} \mathbf{p}(t), \quad (3.1)$$

where \mathbf{L} presents the transition matrix. A formal solution is

$$\mathbf{p}(t) = e^{\mathbf{L}t} \mathbf{p}(t'=0). \quad (3.2)$$

The matrix element $(e^{\mathbf{L}t})_{ij}$ of the evolution operator is to be identified with the conditional probability of finding the system in state i at time t provided it has been in state j at time $t'=0$. The equilibrium distribution is \mathbf{p}_0 and obeys

$$\mathbf{L} \mathbf{p}_0 = 0. \quad (3.3)$$

\mathbf{L} is nonsymmetric. The left eigenvector of \mathbf{L} corresponding to the eigenvalue zero is $\mathbf{1}^T = (1, 1, \dots)$.

We consider observables $M(t)$ presented as

$$M(t) = \langle \mathbf{f} \mathbf{g}_0 \rangle = \mathbf{f}^T e^{\mathbf{L}t} \mathbf{g}, \quad (3.4)$$

$$g_i = g_{0i} p_i(t'=0). \quad (3.5)$$

Such observables measure the correlation between property \mathbf{f} at time t and property \mathbf{g}_0 at time $t'=0$, averaged over the distribution $\mathbf{p}(t'=0)$. In case \mathbf{f} is identical with \mathbf{g}_0 and $\mathbf{p}(t'=0) = \mathbf{p}_0$, $M(t)$ is an equilibrium autocorrelation function. In the following we consider only the deviation of $M(t)$ from the equilibrium value assumed asymptotically ($t \rightarrow \infty$)

$$\begin{aligned} \Delta M(t) &= M(t) - M(t \rightarrow \infty) \\ &= \langle \mathbf{f} \mathbf{g}_0 \rangle - \langle \mathbf{f} \rangle \langle \mathbf{g}_0 \rangle \\ &= \mathbf{f}^T e^{\mathbf{L}t} \mathbf{g} - \sum_i f_i p_{0i} \sum_j g_{0j} p_j(t'=0). \end{aligned} \quad (3.6)$$

To derive a more convenient expression for $\Delta M(t)$ we introduce a projection operator \mathbf{J}_0 given by the dyadic product $\mathbf{p}_0 \mathbf{1}^T = \lim_{t \rightarrow \infty} e^{\mathbf{L}t}$, which projects onto the equilibrium distribution \mathbf{p}_0 . $(1 - \mathbf{J}_0)$ is then the projection operator onto the orthogonal complement of \mathbf{p}_0 . $(1 - \mathbf{J}_0)$ applied to a vector \mathbf{g} yields

$$\mathbf{g}' = (1 - \mathbf{J}_0) \mathbf{g} = \mathbf{g} - \mathbf{p}_0 \sum_i g_i. \quad (3.7)$$

The sum of the components of \mathbf{g}' vanishes, hence, \mathbf{g}' is orthogonal to 1^T . We see from (3.6), that a vector \mathbf{g} , projected by $(1 - \mathbf{J}_0)$, leads to an observable $M(t)$ with a vanishing equilibrium value $M(\infty)$. The operators \mathbf{L} and \mathbf{J}_0 commute and we can rewrite (3.6)

$$\Delta M(t) = \mathbf{f}^T (1 - \mathbf{J}_0) e^{\mathbf{L}t} (1 - \mathbf{J}_0) \mathbf{g}. \quad (3.8)$$

Equation (3.8), or rather its Laplace transform

$$\begin{aligned} \Delta \tilde{M}(\omega) &= \int_0^\infty dt e^{-\omega t} \Delta M(t) \\ &= \mathbf{f}^T (1 - \mathbf{J}_0) \frac{1}{\omega - \mathbf{L}} (1 - \mathbf{J}_0) \mathbf{g} \end{aligned} \quad (3.9)$$

is the starting point of the GME. $\Delta \tilde{M}(\omega)$ can be expanded about $\omega = 0$ and $\omega = \infty$

$$\Delta \tilde{M}(\omega) \sim \sum_{\nu=0}^{\infty} \mu_{-\nu-1} (-\omega)^\nu, \quad \text{as } \omega \rightarrow 0, \quad (3.10)$$

$$\Delta \tilde{M}(\omega) \sim \frac{1}{\omega} \sum_{\nu=0}^{\infty} \mu_\nu \left[\frac{-1}{\omega} \right]^\nu \quad \text{as } \omega \rightarrow \infty. \quad (3.11)$$

The expansion coefficients are the generalized moments μ_ν

$$\mu_\nu \equiv (-1)^\nu \mathbf{f}^T \mathbf{L}^\nu \mathbf{g}. \quad (3.12)$$

The moments can also be expressed through $\Delta M(t)$. One finds

$$\left. \frac{\partial^\nu}{\partial t^\nu} \right|_{t=0} \Delta M(t) = (-1)^\nu \mu_\nu, \quad \nu = 0, 1, \dots, \quad (3.13)$$

$$\int_0^\infty dt t^\nu \Delta M(t) = \nu! \mu_{-\nu-1}, \quad \nu = 0, 1, \dots \quad (3.14)$$

The moments for $\nu \geq 0$ are referred to as high-frequency moments. The moments for $\nu < 0$ correspondingly are called low-frequency moments and weigh the long-time behavior of $\Delta M(t)$. μ_0 is the initial value $\Delta M(0)$.

The GME approximates $\Delta M(\omega)$ by an $[N-1, N]$ Padé approximant $\Delta \tilde{m}(\omega)$, which is chosen as to reproduce a desired number of terms of the low- and the high-frequency expansion (3.10) and (3.11), respectively. The mathematical conditions under which such a two-sided Padé approximant exists have been investigated.³⁷⁻³⁹ This approximant can be written in the form

$$\Delta \tilde{M}(\omega) \approx \Delta \tilde{m}(\omega) = \sum_{n=1}^N \frac{a_n}{\lambda_n + \omega}. \quad (3.15)$$

We require $\Delta \tilde{m}(\omega)$ to reproduce N_h high- and N_l low-frequency moments ($N_h + N_l = 2N$) of the exact observable $\Delta \tilde{M}(\omega)$ and will refer to it as $[N_h, N_l]$ approximant. In the time domain $\Delta \tilde{m}(\omega)$ corresponds to a sum of exponentials

$$\Delta M(t) \approx \Delta m(t) = \sum_{n=1}^N a_n e^{-\lambda_n t}. \quad (3.16)$$

The connection between the a_n and λ_n on one side and the moments on the other side is given by the $2N$ relations

$$\begin{aligned} \sum_{n=1}^N a_n \lambda_n^\nu &= \mu_\nu, \\ \nu &= -N_l, -N_l + 1, \dots, N_h - 2, N_h - 1. \end{aligned} \quad (3.17)$$

In case of a $[1, 1]$ approximation (3.17) yields

$$a_1 = \mu_0, \quad \lambda_1 = \frac{\mu_0}{\mu_{-1}}. \quad (3.18)$$

In case $N=2$ the solution is obtained by the algorithm⁴⁰ ($-N_l = m$)

$$\begin{aligned} x &= \mu_{m+1}^2 - \mu_{m+2} \mu_m, \\ y &= \mu_{m+2} \mu_{m+1} - \mu_{m+3} \mu_m, \\ z &= \mu_{m+2}^2 - \mu_{m+3} \mu_{m+1}, \\ \lambda_1 &= [y + (y^2 - 4xz)^{1/2}] / (2x), \end{aligned} \quad (3.19)$$

$$\lambda_2 = [y - (y^2 - 4xz)^{1/2}] / (2x), \quad (3.20)$$

$$a_1 = (\lambda_2 \mu_{m+2} - \mu_{m+3}) / [\lambda_1^{m+2} (\lambda_2 - \lambda_1)], \quad (3.21)$$

$$a_2 = (\lambda_1 \mu_{m+2} - \mu_{m+3}) / [\lambda_2^{m+2} (\lambda_1 - \lambda_2)]. \quad (3.22)$$

In case $N > 2$ the solution of (3.17) for numerical purposes is best expressed as an equivalent eigenvalue problem.^{29,30}

The GME is based on the availability of the moments μ_ν . The high-frequency moments ($\nu \geq 0$) can be obtained by applying to $(1 - \mathbf{J}_0) \mathbf{g}$ the operator \mathbf{L}^ν and multiplying the result by \mathbf{f}^T . For the low-frequency moments ($\nu < 0$) one needs to evaluate recursively

$$\mathbf{g}'_1 = (1 - \mathbf{J}_0) \mathbf{L}^{-1} (1 - \mathbf{J}_0) \mathbf{g}, \quad \mu_{-1} = \mathbf{f}^T \mathbf{g}'_1, \quad (3.23)$$

$$\begin{aligned} \mathbf{g}'_2 &= (1 - \mathbf{J}_0) \mathbf{L}^{-1} \mathbf{g}'_1, \quad \mu_{-2} = \mathbf{f}^T \mathbf{g}'_2 \\ &\vdots \end{aligned} \quad (3.24)$$

Since \mathbf{L} is nonsingular in the subspace onto which $(1 - \mathbf{J}_0)$ projects (we assume that the null space of \mathbf{L} is the single-equilibrium state \mathbf{p}_0 which is true as long as \mathbf{L} is ergodic, i.e., connects all spin configurations) the singularity of \mathbf{L} does not affect the solution of (3.23), (3.24). However, for a numerical solution one may rather adapt the following scheme³⁴: First construct a matrix $\hat{\mathbf{L}}$ and a state $\hat{\mathbf{g}}$ by reducing the dimension of \mathbf{L} and \mathbf{g} by one through elimination of, say, the last row and column of \mathbf{L} and the corresponding element of \mathbf{g} ; solve the reduced equation

$$\hat{\mathbf{L}} \hat{\mathbf{g}}_1 = \hat{\mathbf{g}}, \quad (3.25)$$

fill in a zero for the eliminated component of \mathbf{g}_1 , and obtain \mathbf{g}'_1 in the orthogonal subspace by applying the projector $(1 - \mathbf{J}_0)$; continue this way for all remaining \mathbf{g}'_i .

We have chosen the following procedure to evaluate the transition-rate matrix \mathbf{L} for the kinetic Ising model. A spin system consisting of N spins has a state space of dimension 2^N . Hence, \mathbf{L} is represented by a $2^N \times 2^N$ matrix. The elements of \mathbf{L} are either w_{par} , w_{antipar} , or w_{mix} [see (2.4)–(2.6)] for allowed, i.e., single-spin flip, transitions and vanish for all other transitions. An efficient method to assign the proper values to the elements of \mathbf{L} is

based on an ordering of the spin configurations such that the i th spin configuration is given by the binary representation of i , a 1 implying spin-up, and a 0, spin down. An example for a chain of six spins would be that the state $i=14$ with the binary representation 001110 corresponds to the spin configuration $\downarrow\downarrow\uparrow\uparrow\uparrow\downarrow$.

Let us now consider all transition rates in the i th row of \mathbf{L} . We first consider all numbers j_l which differ from i in their binary representation by a single digit, i.e., represent spin configurations which can be reached from the i th configuration through a single-spin flip. We then set $L_{i,j}=0$ except for $j \in \{j_1, j_2, \dots, j_N\}$. To attribute the correct value w_{par} , w_{antipar} , or w_{mix} to L_{i,j_l} one needs to compare the binary digits of i at positions $l-1$, l , and $l+1$, when l is the position in which the binary representations of i and j_l differ. After one has filled all off-diagonal positions of \mathbf{L} one obtains the diagonal element on account of the conservation of probability, i.e.,

$$L_{i,i} = - \sum_{j (j \neq i)} L_{i,j}. \quad (3.26)$$

The resulting matrix \mathbf{L} has 2^N elements in each row but only $N+1$ of these are nonvanishing, i.e., \mathbf{L} is a "sparse" matrix. For the solution of the sparse linear equations (3.25) we used the package Itpack 2C⁴¹ which relies on adaptive accelerated iterative algorithms. Of the subroutines supplied with this package we found the RSCG code to match our needs best.

IV. RESULTS FOR THE ONE-DIMENSIONAL MODEL

A. Relaxation of correlation functions for $\delta=0$

As a first observable we consider the spin autocorrelation function $C_N(t)$ in the special case $\delta=0$. The analytical solution for $C_N(t)$ is known in this case [Eq. (2.14)] and provides a test for the accuracy of the GME.

In Fig. 1 the exact $C_N(t)$ and its [3,3] GME are compared for rings of different length N . The close agreement shows that an expansion based on three low- and three high-frequency moments is sufficient to reproduce $C_N(t)$. Figure 1 demonstrates also that the spin autocorrelation relaxes more slowly in smaller rings.

Next we consider the magnetization correlation function

$$\langle M(t)M(0) \rangle = \sum_{i,j=1}^N \langle \sigma_i(t)\sigma_j(0) \rangle. \quad (4.1)$$

The relaxation of the magnetization in finite rings was determined earlier³ to be monoexponential:

$$M(t) = M(0)e^{-\alpha(1-\gamma)t}. \quad (4.2)$$

Hence, the magnetization correlation function is monoexponential as well

$$\langle M(t)M(0) \rangle = \langle M(0)M(0) \rangle e^{-\alpha(1-\gamma)t}. \quad (4.3)$$

The [1,1] GME yields this relaxation time exactly. If, for example, a [2,2] GME is attempted, the corresponding moments in Eqs. (3.19)–(3.22) yield vanishing x , y , and z . If one attempts a [3,3] GME the eigenvalue routine need-

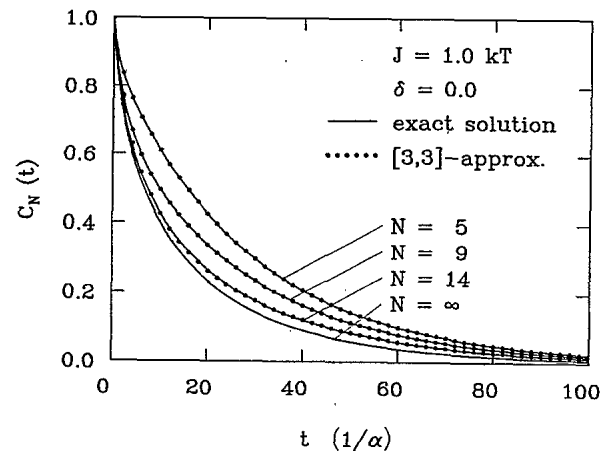


FIG. 1. Comparison of [3,3] GME and of exact description for the spin autocorrelation function $C_N(t)$ in rings of different length N , the latter are evaluated according to Eqs. (2.14) and (2.13).

ed to determine a_n and λ_n (Refs. 29 and 30) does not converge.

B. Glauber dynamics for $\delta \neq 0$

In the preceding section we found for $\delta=0$ that the GME reproduces well the spin autocorrelation function and the magnetization correlation function. We want to consider now the spin autocorrelation function $C_N(t)$ for $\delta \neq 0$. An exact analytic solution does not exist for $C_N(t)$ in this case. We determine first the most simple approximation to $C_N(t)$, namely its [1,1] GME. This approximation can be represented as

$$C_N(t) \approx C_N(0) \exp \left[- \frac{t}{\tau_{[1,1]}} \right], \quad (4.4)$$

where $\tau_{[1,1]}$ can be interpreted as the mean relaxation time. In Fig. 2 the δ dependence of $\tau_{[1,1]}$ is shown. We find $\tau_{[1,1]}$ to be rather constant in the center part of the δ interval $[-1,1]$, but to increase towards the boundaries.

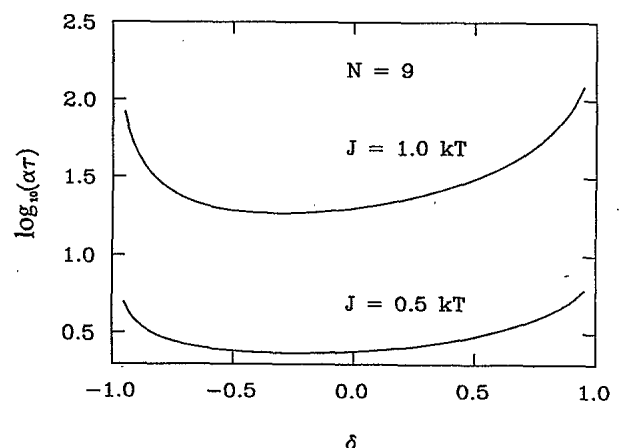


FIG. 2. Mean relaxation time $\tau_{[1,1]}$ as a function of δ in a ring consisting of 9 spins; $\tau_{[1,1]}$ is shown for two coupling constants J .

An increase of the coupling strength J/kT causes an increase of the relaxation time. This effect will be discussed further in Sec. IV C below.

1. Nonergodic behavior for $\delta \rightarrow -1$

With δ approaching -1 the rates w_{par} and w_{antipar} vanish and the corresponding spin flips become forbidden. These spin flips alter the energy of the system, i.e., in the limit $\delta \rightarrow -1$ the energy remains constant. The space of all spin configurations is then divided into equal energy subspaces, which are not linked by the dynamics, i.e., the system becomes nonergodic. The eigenvalue $\lambda=0$ of L becomes degenerate and an equilibrium state exists for each subspace. In a system with N spins, N even, there are $N/2$ constant energy subspaces [$(N-1)/2$ for N odd]. For that reason the GME, which requires the inversion of $(1-J_0)L(1-J_0)$ in the course of solving Eq. (3.23) cannot be applied. However, we like to argue that an application of the GME near $\delta=-1$ should reveal a most interesting behavior of the spin system, namely a slowing down of relaxation processes due to the emergence of nonergodicity.

Close to $\delta=-1$, relaxation of any observable takes place first within each constant energy subspace. After quasiequilibrium within each such subspace is reached, relaxation between the different subspaces takes place on a much slower time scale. This behavior of relaxation on very distinct time scales can be reproduced well by the GME, but not by conventional expansions based solely on high-frequency moments. As a demonstration we compare in Fig. 3 the [3,3] GME with a [6,0] GME, the latter being based on the moments $\mu_0, \mu_1, \dots, \mu_5$. The [6,0] GME describes solely the initial phase of the relaxation correctly, but fails to account properly for the late phase, which corresponds to the slowly decaying component of the [3,3] description.

In order to test the validity of the GME we construct an alternative description of the slow-relaxation phase. This description derives from the fact that the initial fast

relaxation leads to quasiequilibria within the equal-energy subspaces. If the quasiequilibrium value of an observable $\Delta M(t)$ inside a particular subspace vanishes as, of course, the long-time equilibrium value does, then this subspace will not contribute to the slow second component, since the observable has fallen off to its final value already. In case of the spin autocorrelation function and an initial distribution $\mathbf{p}(t'=0)=\mathbf{p}_0$, the only quasiequilibrium equal-energy subspaces that contribute a nonvanishing term to the slow-relaxation phase are the ones with all spins up and with all spins down. Both subspaces consist of just one state. Even though these two states have the same energy, they are not linked by transitions of the w_{mix} type. All other equal-energy subspaces are symmetric in the sense that for each state the subspace contains also the inverse state (with all spins flipped). Therefore, the observable considered has vanishing quasiequilibrium values in all subspaces except the two spaces with all spins parallel.

We express the separation of fast and slow contributions to $C_N(t)$ by

$$C_N(t) = (1 - a_{\text{slow}})C_{\text{fast}}(t) + a_{\text{slow}}e^{-t/\tau_{\text{slow}}}, \quad (4.5)$$

where $C_{\text{fast}}(t)$ describes the fast relaxation [$C_{\text{fast}}(0)=1$, $C_{\text{fast}}(t \rightarrow \infty)=0$]. We refer to τ_{slow} as the relaxation time of the slow phase and to a_{slow} as the respective amplitude. Since in the two all-parallel subspaces the expectation value of the spin correlation function is $\langle \sigma_i^2 \rangle = 1$, the amplitude a_{slow} is twice the thermal equilibrium probability of being in an all-parallel state, i.e.,

$$a_{\text{slow}} = \frac{2}{Z_N} e^{NJ/kT} = \frac{2}{(1 + e^{-2J/kT})^N + (1 - e^{-2J/kT})^N} \quad (4.6)$$

with Z_N being the partition function of the one-dimensional N -spin model. Even though the rate w_{par} is small, if δ is close to -1 , each of the N spins in an all-parallel state can flip according to w_{par} and, in this way, establish the connection to the other subspaces. Hence, the relaxation time τ_{slow} is given by

$$\tau_{\text{slow}} = \frac{1}{w_{\text{par}}(\delta, \gamma)N} = \frac{2}{\alpha(1+\delta)(1-\gamma)N} \quad (4.7)$$

The minimal GME, which can resolve two distinct relaxation processes, is the [2,2] approximation. We find excellent agreement between the above estimates of τ_{slow} and a_{slow} on the one hand and $\tau_{[2,2],1}$ and $a_{[2,2],1}$ for the slower of the two exponentials in the [2,2] GME, on the other hand. Some data are presented in Table II. The table shows, in particular, for $N=10$ and $J=0.5kT$ in how far the approximation (4.5) improves as δ approaches -1 .

In case of the magnetization correlation function there is a slow component as well. The arguments given above lead to the same relaxation time τ_{slow} , but the amplitude a_{slow} has to be multiplied by a factor of N^2 , because the all-parallel states contribute comparatively more to the magnetization correlation than to the spin autocorrelation.

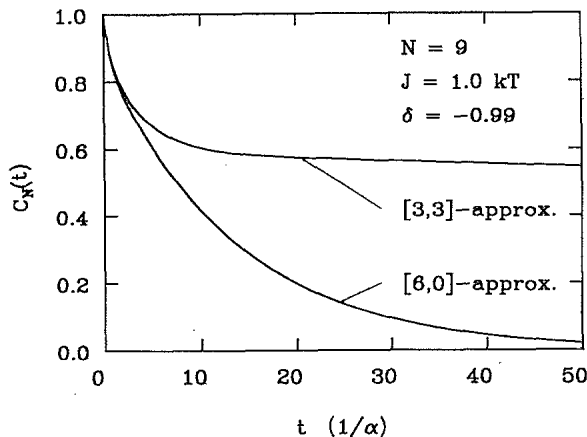


FIG. 3. Comparison of a [3,3] and a [6,0] description for the spin autocorrelation function $C_N(t)$ in a ring consisting of 9 spins.

TABLE II. Amplitude and relaxation time of the slow component of the spin autocorrelation function $C_N(t)$ in the limit $\delta \rightarrow -1$ as evaluated by means of the [2,2] GME ($\tau_{[2,2],1}, a_{[2,2],1}$) and by means of Eqs. (4.6) and (4.7).

$J(kT)$	δ	N	$\tau_{[2,2],1}(\alpha^{-1})$	$\tau_{\text{slow}}(\alpha^{-1})$	$a_{[2,2],1}$	a_{slow}
0.5	-0.9999	6	13 978.0	13 982.0	0.3027	0.3024
1.0	-0.9999	6	92 672.0	92 664.0	0.7814	0.7814
0.5	-0.99	10	72.5	83.9	0.1316	0.0872
0.5	-0.999	10	823.2	839.0	0.0915	0.0872
0.5	-0.9999	10	8 373.0	8 390.5	0.0876	0.0872
0.5	-0.99999	10	83 893.0	83 905.0	0.0872	0.0872
1.0	-0.9999	10	55 607.0	55 598.0	0.5275	0.5274
0.5	-0.9999	14	5 893.0	5 932.0	0.0258	0.0249
1.0	-0.9999	14	39 716.0	39 713.0	0.3310	0.3310

tion function.

The possibility to observe the nonergodicity discussed above is limited to finite systems, since the amplitude a_{slow} falls off quickly with growing system size. On the other hand, since a_{slow} increases with J/kT , for each finite number of spins one can find a (possibly huge) coupling strength J/kT such that nonergodicity occurs.

2. Nonergodic behavior for $\delta \rightarrow +1$

When δ approaches the value $+1$, w_{mix} vanishes. As in the case $\delta \rightarrow -1$, dynamical decoupling of the state space occurs and nonvanishing quasiequilibrium values of observables within the subspaces lead to slow components of the relaxation functions. Because successive creation and annihilation of Bloch domains can move Bloch walls in steps of two lattice spacings [see (2.11)], the decomposition pattern into subspaces is length dependent and complicated. We do not want to further elaborate on this point here.

C. Critical dynamical exponents

Figure 2 demonstrates that the relaxation of $C_N(t)$ slows down for increasing values of the coupling strength J/kT , i.e., for decreasing temperature. In this section we consider the slowing down of the magnetization correlation function near $T=0$ and infer from Eq. (4.3) that the relaxation time for this observable in case $\delta=0$ diverges like

$$\tau \propto e^{4J/kT}, \text{ for } J/kT \rightarrow \infty. \quad (4.8)$$

In the same limit the static correlation length ξ [compare Eq. (2.2)] diverges like

$$\xi \propto e^{2J/kT}, \text{ for } \frac{J}{kT} \rightarrow \infty. \quad (4.9)$$

The relaxation time diverges as some power of ξ , the exponent z connecting τ and ξ is called the critical dynamical exponent. z depends on the choice of transition rates. In case $\delta=0$ Eqs. (4.8) and (4.9) yield a relation

$$\tau \propto \xi^2, \quad (4.10)$$

i.e., an exponent $z=2$ (see Ref. 8).

This exponent is recovered by the GME not only for vanishing δ but for a wide range of δ values, provided δ is kept independent of J . To reach this result, we computed the mean relaxation time $\tau_{[1,1]}$ as defined in Sec. IV B for the magnetization correlation function in finite rings and compare it to the static correlation length ξ for the infinite system. We found z to be rather independent of the length.

For a J -dependent δ value

$$\delta = \frac{\gamma}{2-\gamma} \quad (4.11)$$

which amounts to $w_{\text{mix}} = w_{\text{par}}$ Dekker and Haake⁹ as well as Kimball¹⁰ found $z=4$ in case of an infinite spin chain. The same exponent had been determined by Pandit, Forgacs, and Rujan for finite rings.¹³ We have tested the critical behavior for finite rings with $N=5$ and $N=12$ by choosing δ according to (4.11) and increasing J/kT . In Fig. 4 we compare ξ and the mean relaxation time $\tau_{[1,1]}$ of the magnetization correlation function. The slope of $\tau(\xi)$ in a log-log plot corresponds to $z=4$, i.e., finite and infinite rings agree in this respect. Of course, this treatment could be improved if one would represent the

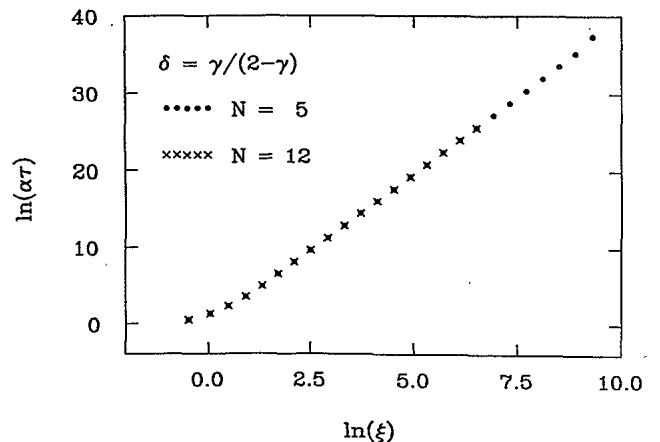


FIG. 4. Mean relaxation time $\tau_{[1,1]}$ of the magnetization correlation function as a function of the static correlation length ξ in the infinite system. δ depends on J according to Eq. (4.11). The slope of the line amounts to $\tau \propto \xi^4$.

abscissa in Fig. 4 by ξ_N as determined by finite-size scaling. However, the fact that $\tau(\xi)$ in Fig. 4 appears to coincide for $N=5$ and $N=12$ suggests that finite-size scaling is not essential in this particular situation.

In Sec. IV B we described a slow phase of the spin autocorrelation function as well as of the magnetization correlation function in the limit $\delta \rightarrow -1$. The slow phase resulted from a dynamical decomposition of the spin configuration space into subspaces, i.e., from nonergodicity. We characterized this phase in terms of a relaxation time τ_{slow} and an amplitude (for the spin autocorrelation function) a_{slow} . Clearly τ_{slow} will increase for increasing coupling strength. If we connect δ and J through

$$\delta = \frac{-\gamma}{2-\gamma}, \quad (4.12)$$

then τ_{slow} diverges like

$$\tau_{\text{slow}} = \frac{2}{\alpha \left[1 - \frac{\gamma}{2-\gamma} \right] (1-\gamma)N} \sim \frac{1}{4N} e^{8J/kT} \text{ for } \frac{J}{kT} \rightarrow \infty, \quad (4.13)$$

which yields again an exponent $z=4$. The relaxation time τ_{slow} for $\delta \rightarrow -1$ is inversely proportional to the number of spins N . Furthermore, the corresponding amplitude a_{slow} vanishes exponentially with growing N . Therefore, the occurrence of the slow phase and the critical dynamical exponent $z=4$ are finite-size effects limited to small systems.

D. Williams-Watts description of the correlation functions

The time dependence of observables of photon correlation spectroscopy experiments as well as dielectric relaxation experiments on polymers is often interpreted in terms of the Williams-Watts function Eq. (1.1).²¹⁻²³ The good agreement between experimental data and this empirical function motivated the search for a simple physical model which yields relaxation functions of the Williams-Watts type. Skinner²⁶ examined the (infinite) one-dimensional Ising model in the limiting case $\delta = -1$. He determined the spin autocorrelation function, which turned out to be of Williams-Watts type with an exponent $\beta=0.5$. By numerical Laplace transformation of the spin-spin correlation function he further calculated a magnetization correlation function which could be fitted well by a Williams-Watts function with $\beta=0.74$. Budimir and Skinner²⁷ examined the Glauber model for $\delta=0, \pm 1$ by means of a continued fraction approximation to the spin autocorrelation function. Since this approach is equivalent to a high-frequency expansion, the results can be trusted only in the short-time domain and the authors determined numerically a cutoff time up to which the evaluated correlation functions are reliable. Again their solutions could be well fitted in the specified time domain by Williams-Watts functions with values for β between 0.648 and 1.

Since we are considering the same observables as Budimir and Skinner, with the sole difference that our systems are finite, we test our relaxation functions for Williams-Watts type behavior and compare the exponent β to Budimir and Skinner's results. This behavior does not apply in a strict mathematical sense since finite stochastic systems with first-order kinetics can always be represented through a series of exponential decays. The behavior can only be verified within certain error bounds, i.e., the attitude in our paper is that the Williams-Watts function is merely an expression which encapsulates well certain multiexponential decays.

In order to obtain the Williams-Watts parameters a , τ , and β we modify our expansion scheme. Instead of approximating the observable by a sum of exponentials we approximate it by a Williams-Watts function. This amounts to replacing Eq. (3.16) by

$$\Delta M(t) \approx \Delta w(t) = a \exp \left[- \left[\frac{t}{\tau} \right]^\beta \right]. \quad (3.16')$$

For a Williams-Watts function only μ_0 and the long-time moments $\mu_{-\nu}$ exist [see Eqs. (3.13) and (3.14)]. The latter are related to a , τ , and β through

$$\begin{aligned} \mu_{-\nu-1} &= \frac{a}{\nu!} \int_0^\infty dt t^\nu \exp \left[- \left[\frac{t}{\tau} \right]^\beta \right] \\ &= \frac{a}{\nu!} \frac{\tau^{\nu+1}}{\beta} \Gamma \left[\frac{\nu+1}{\beta} \right]. \end{aligned} \quad (4.14)$$

We require that $\Delta M(t)$ and $\Delta w(t)$ agree with respect to the moments μ_0 , μ_{-1} , and μ_{-2} . Then the relations (3.17) have to be replaced by

$$\mu_0 = a, \quad (4.15)$$

$$\mu_{-1} = \frac{a\tau}{\beta} \Gamma \left[\frac{1}{\beta} \right], \quad (4.16)$$

$$\mu_{-2} = \frac{a\tau^2}{\beta} \Gamma \left[\frac{2}{\beta} \right]. \quad (4.17)$$

Numerical solution of the nonlinear system of equations (4.15)–(4.17) yields a , τ , and β in an unambiguous way. Equations (4.15)–(4.17) provide a simple and systematic description of a multiexponential decay in terms of a Williams-Watts function. It is the optimal description in case the whole time regime is taken into account. We note, however, that if a Williams-Watts function is fitted to an observable only in a finite-time interval there may be discrepancies with our approach.

In order to test the variant of the GME established by Eqs. (3.16') and (4.14)–(4.17) we consider the spin autocorrelation function $C_N(t)$ for the case with known analytical solution, i.e., $\delta=0$ [see Eq. (2.14)]. μ_{-1} and μ_{-2} can be obtained by integration according to Eq. (3.14). We find

$$\mu_{-1} = \frac{1}{\alpha(1-\gamma^2)} + \frac{2N}{\alpha(1-\gamma^2)^{1/2} \left[\left(\frac{1+(1-\gamma^2)^{1/2}}{\gamma} \right)^N - \left(\frac{1-(1-\gamma^2)^{1/2}}{\gamma} \right)^N \right]}, \quad (4.18)$$

$$\begin{aligned} \mu_{-2} = & \frac{\gamma^2+2}{2\alpha^2(1-\gamma^2)^2} + \frac{3N}{\alpha^2(1-\gamma^2)^{3/2} \left[\left(\frac{1+(1-\gamma^2)^{1/2}}{\gamma} \right)^N - \left(\frac{1-(1-\gamma^2)^{1/2}}{\gamma} \right)^N \right]} \\ & + \frac{N^2}{\alpha^2(1-\gamma^2) \left[\left(\frac{1+(1-\gamma^2)^{1/2}}{\gamma} \right)^N + \left(\frac{\gamma}{1+(1-\gamma^2)^{1/2}} \right)^N - 2 \right]}. \end{aligned} \quad (4.19)$$

In order to compare with the result of Budimir and Skinner for an infinite ring we take the limit $N \rightarrow \infty$

$$\mu_{-1} = \frac{1}{\alpha(1-\gamma^2)}, \quad (4.20)$$

$$\mu_{-2} = \frac{\gamma^2+2}{2\alpha^2(1-\gamma^2)^2}. \quad (4.21)$$

In Fig. 5 the exact solution, Budimir and Skinner's Williams-Watts fit and an approximation based on $\mu_0=1$, μ_{-1} , and μ_{-2} as given by (4.20) and (4.21) are shown. Both approximations are in good agreement with the exact solution. The Williams-Watts parameters are $a=1$, $\tau=11.36\alpha^{-1}$, $\beta=0.675$ (Budimir and Skinner) and $a=1$, $\tau=11.65\alpha^{-1}$, $\beta=0.732$ (GME).

We like to investigate how for the spin autocorrelation function the choice of transition rates, i.e., of δ , influences the Williams-Watts exponent β . Figure 6 presents β for the whole range of δ values. Typical values of β lie between 0.75 and 0.8. The decrease of β below 0.75 near $\delta=-1$ is connected with the onset of nonergodicity which results in a slow-relaxation phase. We found that for $J \leq 0.5kT$ the Williams-Watts representation agrees well with the [3,3] GME, i.e., with the numerically

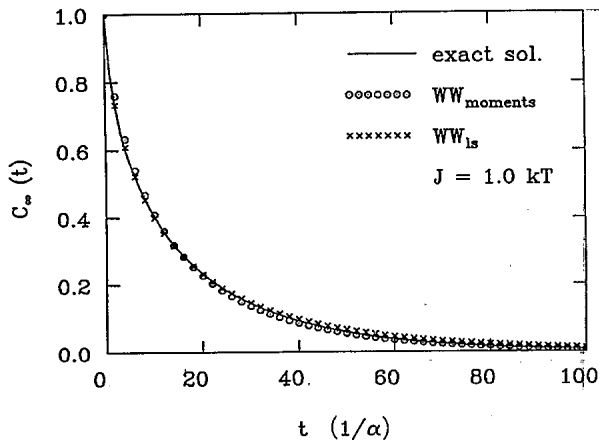


FIG. 5. Relaxation of the spin autocorrelation function $C_\infty(t)$ for $J=1.0kT$. The exact solution is compared to Williams-Watts functions which result from a least-squares fit to a short-time continued fraction approximation (WW_{ls}) and from a modified GME based on the moments μ_0 , μ_{-1} , and μ_{-2} ($WW_{moments}$).

exact spin autocorrelation, for all δ values except near the boundaries ± 1 where finite-size effects become important. For $J > 0.5kT$ the correlation length ξ is so large that finite-size effects are always important and the Williams-Watts description fails.

The Williams-Watts exponent β for the magnetization correlation function for the whole range of δ values is shown in Fig. 7. For $\delta=0$ the relaxation of $\langle M(t)M(0) \rangle$ is strictly monoexponential [see Eq. (4.3)], hence, for all coupling constants J holds $\beta=1$. In the range $[-0.8, 0.95]$ the correlation functions for the J values considered remain rather monoexponential and can be approximated well by Williams-Watts functions with $\beta > 0.9$. For such values of β the nonexponential character of the correlation function is not very distinct. Close to the boundaries the slow phases and nonergodicity determine the relaxation process and the relaxation function are not of the Williams-Watts form.

V. EFFECTIVE RATE CONSTANTS AND REDUCED TRANSITION MATRIX

A. One-dimensional systems

The GME has the advantage of a free choice of transition rates and of a numerical effort which does not diverge as relaxation times increase. The advantages come at the price of a restriction to finite systems. The accessible system size N is determined by the dimension d of the transition matrix L and, actually, is rather small.

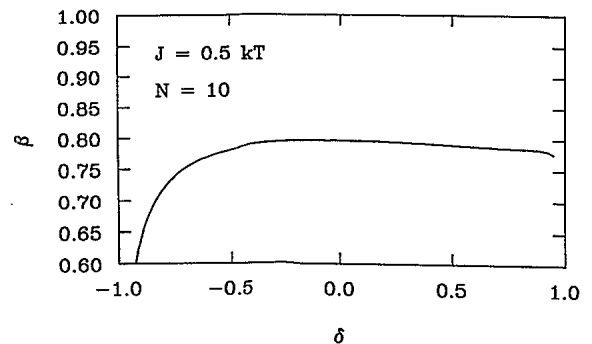


FIG. 6. Parameter β as a function of δ for $J=0.5kT$ of a Williams-Watts description of the spin autocorrelation function. The Williams-Watts parameters were determined from μ_0 , μ_{-1} , and μ_{-2} .

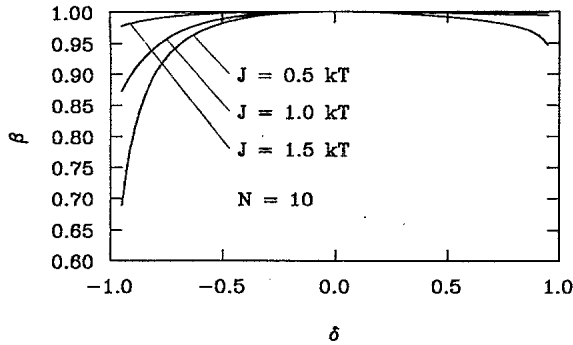


FIG. 7. As in Fig. 6, but for the magnetization correlation function.

In order to describe correlation functions $\langle O(t)O(0) \rangle$ for larger systems we collect individual spin configurations into subsets of configurations such that the observable O assumes identical values for all configurations in a subset. We require that a flip of a single spin necessarily introduces a transition to a different subset. We then derive an approximate description which disregards variations of the distribution inside the chosen subsets and considers only transitions between subsets. These transitions are described by the "effective rate constants."

The observable suitable for this idea is the magnetization $M = \sum_{i=1}^N \sigma_i$. M takes on the same value M_k for many different spin configurations which are collected

correspondingly into subsets. The flip of any single spin causes M to change, i.e., there are no transitions within a subset. The energy of the system is an example of an observable which is not suitable for the introduction of effective rates because there are energy conserving spin flips.

In the following we consider, therefore, the magnetization correlation function $\langle M(t)M(0) \rangle$. In a system of N spins the maximum and minimum value of M is $+N$ and $-N$, respectively. Because any spin flip changes the magnetization by ± 2 units, M assumes $N+1$ different values M_k ,

$$M_k = -N, -N+2, \dots, N-2, N. \quad (5.1)$$

Correspondingly there are only $N+1$ subsets of spin configurations with equal magnetization. For the sake of simplicity we denote these subsets by the same symbol M_k as the value of M in this subset. i and j denote states in the full configuration space. With $M(i)$ being the magnetization of state i , the equilibrium probability for M_k being populated is

$$p_0(M_k) = \sum_{i \in [M(i)=M_k]} p_0(i). \quad (5.2)$$

The effective rate for transition from subset M_k to subset M_k-2 is

$$w(M_k \rightarrow M_k-2) = \frac{1}{p_0(M_k)} \sum_{\substack{i,j \\ [M(i)=M_k, M(j)=M_k-2]}} w(i \rightarrow j) p_0(i). \quad (5.3)$$

The inverse rates $w(M_k-2 \rightarrow M_k)$ can be obtained from the principle of detailed balance. We can then construct for the intersubstate kinetics the "reduced" transition matrix L_{red} . Working with L_{red} instead of L , we can apply the GME to the magnetization correlation function as we did in the full state space. The suggested approximation decreases the dimension of the transition matrix from 2^N for L to $N+1$. L_{red} has tridiagonal form and, hence, the long-time moments μ_{-v} are easy to obtain.³² The moments μ_0 and μ_{+1} of the magnetization correlation function are reproduced exactly by the effective rate approximation.

To establish L_{red} the sum in Eq. (5.3) has to be carried out. We note that there are just three distinct values for $w(i \rightarrow j)$: w_{mix} , w_{par} , and w_{antipar} . The equilibrium distribution p_0 can take on only a few values, since the energy E is limited to the range $-NJ \leq E \leq +NJ$ and can only be changed in units of $4J$. Labeling the energy levels $E_1 = -NJ$, $E_2 = (-N+4)J$, ... we need then to determine the numbers $P_N(M_k, E_l)$, $A_N(M_k, E_l)$, and $M_N(M_k, E_l)$ which specify how many transitions of type w_{par} , w_{antipar} , and w_{mix} there are for the spin configurations with energy E_l from the subset M_k to the subset M_k-2 . One can derive the following expressions for these numbers:

$$P_N(M_k, E_l) = \begin{cases} N \begin{bmatrix} \frac{N-M_k}{2} - 1 \\ l-2 \end{bmatrix} \begin{bmatrix} \frac{N+M_k}{2} - 2 \\ l-1 \end{bmatrix}, & \text{if } l \geq 2, \\ 1, & \text{if } l=1, M_k = N-2, \\ 0, & \text{else,} \end{cases} \quad (5.4)$$

$$A_N(M_k, E_l) = \begin{cases} N \begin{bmatrix} \frac{N-M_k}{2} - 1 \\ l-2 \end{bmatrix} \begin{bmatrix} \frac{N+M_k}{2} - 2 \\ l-3 \end{bmatrix}, & \text{if } l \geq 3, \\ 1, & \text{if } l=2, M_k = -N, \\ 0, & \text{else,} \end{cases} \quad (5.5)$$

$$M_N(M_k, E_l) = \begin{cases} 2N \begin{bmatrix} \frac{N-M_k}{2} \\ l-2 \end{bmatrix} \begin{bmatrix} \frac{N+M_k}{2} \\ l-2 \end{bmatrix}, & \text{if } l \geq 2. \\ 0, & \text{if } l = 1. \end{cases} \quad (5.6)$$

With these coefficients we obtain for (5.3)

$$w(M_k \rightarrow M_k - 2) = \sum_{l=1}^{N+1} \frac{p_0(E_l)}{p_0(M_k)} [P_N(M_k, E_l) w_{\text{par}} + A_N(M_k, E_l) w_{\text{antipar}} + M_N(M_k, E_l) w_{\text{mix}}], \quad (5.7)$$

$$p_0(M_k) = \sum_{l=1}^{N+1} [P_N(M_k, E_l) + A_N(M_k, E_l) + M_N(M_k, E_l)] p_0(E_l). \quad (5.8)$$

In Figs. 8(a)–8(d) the GME for the magnetization correlation function in the full state space and in the reduced space are compared. The results from the reduced space agree well with those from the full state space in a major part of the δ interval, particularly, in the region close to the lower bound $\delta = -1$. Only in the limit $\delta \rightarrow +1$ the results in the reduced-state description are poor, since in this limit two successive flip processes [see (2.11)] become important, which are not correctly accounted for by the effective rates.

In Sec. IV B we found a slow component of $\langle M(t)M(0) \rangle$ in the limit $\delta \rightarrow -1$, which should occur in small systems only [see Eqs. (4.6) and (4.7)]. For increasing N the amplitude a_{slow} decreases rapidly. In Fig. 9 $\langle M(t)M(0) \rangle$ is presented for different values of N . The slow component diminishes with increasing N , i.e., it represents a small system effect. Figure 9 demonstrates the high accuracy of the reduced state space approximation in comparison to the GME in the full state space in this parameter regime.

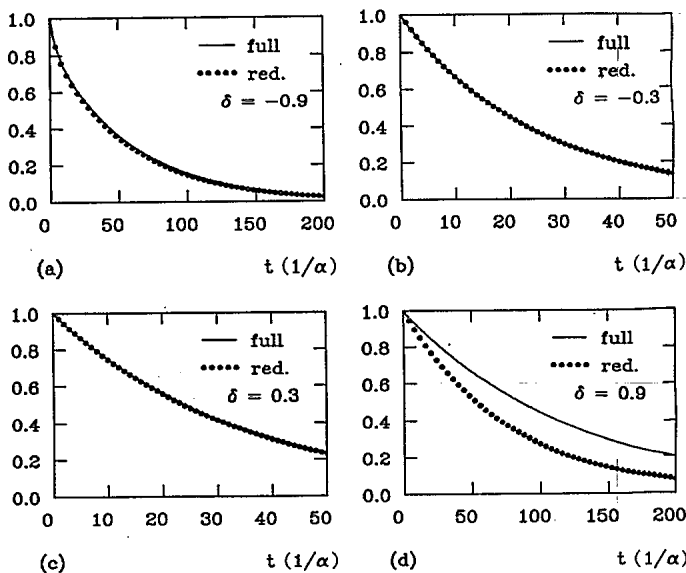


FIG. 8. [3,3] GME of the magnetization correlation function $\langle M(t)M(0) \rangle$ in the reduced state space and in the full state space. The number of spins is $N=12$, the coupling constant $J=1.0kT$.

B. Two-dimensional systems

The GME can also be applied to two-dimensional Ising systems. In the following we will only consider Ising models on a square lattice, although other lattice types could be treated equally well. Our computational resources (MicroVAX II) limited us to 16 spins in a full state-space description. This implies that we can only treat 4×4 square lattices which is very small and allows only to investigate qualitative features of two-dimensional kinetic Ising models. As observables we consider either the magnetization correlation function

$$F(t) = \langle M(t)M(0) \rangle \quad (5.9)$$

or the magnetization intensity correlation function

$$G(t) = \langle M^2(t)M^2(0) \rangle. \quad (5.10)$$

We assumed again periodic boundary conditions. In order to specify the dynamics completely one would have to choose five independent parameters instead of three parameters for the one-dimensional system. We like to

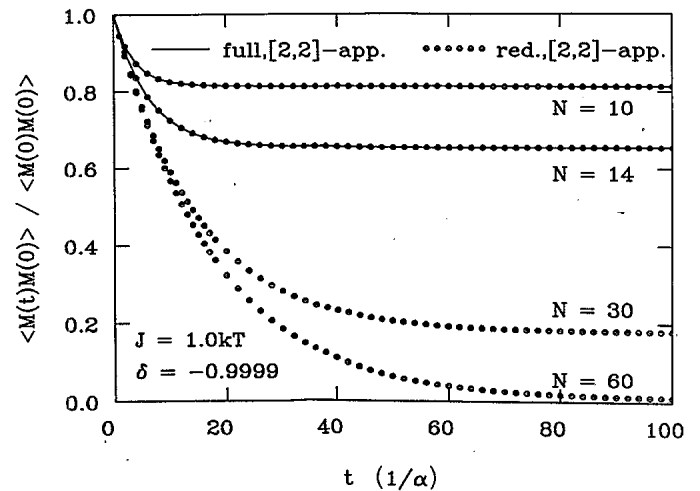


FIG. 9. Comparison of magnetization correlation functions $\langle M(t)M(0) \rangle$ for rings of different size N ($N=10, 14, 30, 60$). For $N=10$ and 14 the correlation functions are evaluated in the full as well as in the reduced space, for $N=30$ and 60 the correlation functions are calculated only in the reduced state space.

avoid the huge number of possible rate constant combinations and rather restrict our study to standard Monte Carlo rates. These are

$$w = \frac{1}{\alpha} \frac{e^{-\delta E/kT}}{1 + e^{-\delta E/kT}}, \quad (5.11)$$

where α specifies the time scale and δE the energy difference between the initial and final states. In order to describe larger systems we applied also the approximation involving a reduced state space of substates collecting spin configurations with identical magnetization M_k . The definition of effective rates is the same as in the one-dimensional case, i.e., Eq. (5.3). For the two-dimensional case, however, we did not succeed to simplify the sum in (5.3) and, hence, were limited to systems with up to 25 spins.

The infinite two-dimensional Ising model has a phase transition at a critical temperature $kT_c = 2.269$ J. Below T_c the spins are oriented preferentially parallel. In the field-free case no orientation is preferred and the expectation value for the magnetization vanishes. In a finite system the transition is smeared out but can still be observed. Below T_c the all-parallel states are by far the most probable states. But the other states are occupied with some small probability and, on a very long time scale, transitions from the all-up state to the all-down state and vice versa occur. On the other hand the initial relaxation process which aligns spins of different orientation takes place on comparatively fast scale. This difference has been described by Stoll, Binder, and Schneider⁴² in connection with a Monte Carlo simulation. The [2,2] GME can resolve these different time scales. In contrast to the Monte Carlo simulation the computing effort does not increase when one of the time scales becomes slower and slower.

In Figs. 10 and 11 the relaxation times $\tau_{[2,2],1}$ and $\tau_{[2,2],2}$ of the [2,2] GME for $F(t)$ are shown as functions of temperature. The relaxation time $\tau_{[2,2],1}$ which can be identified with the slow component of $F(t)$ [Eq. (5.9)] diverges as the temperature becomes lower, because the barrier between the two quasiequilibrium states becomes higher. $\tau_{[2,2],2}$ corresponding to the fast phase also exhibits a slowing down near the critical temperature T_c of the infinite system, however, its value remains finite.

Next we consider the magnetization intensity correlation function $G(t)$. The very slow transitions between the two all-parallel states do not contribute to $G(t)$, and the relaxation process includes the alignment of non-parallel spins only. For this observable we tested the GME by evaluating the operator $e^{L\Delta t}$ numerically and computing the time evolution of the system by applying $e^{L\Delta t}$ to $\mathbf{p}(t'=0)$ successively. This can be done in the 2×2 and 3×3 systems and results in an excellent agreement with the [3,3] GME in either the full- or the reduced-state space as shown in Fig. 12.

Finally we present in Fig. 13 for systems of different sizes the temperature dependence of the mean relaxation time $\tau_{[1,1]}$ of $G(t)$ evaluated in the reduced-state space. The critical slowing down of the relaxation near T_c is found to emerge already for the small systems studied here.

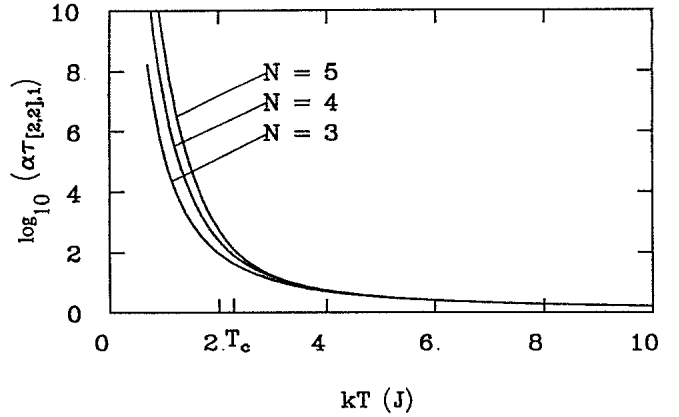


FIG. 10. Relaxation time $\tau_{[2,2],1}$ of the [2,2] GME in the reduced state space for the magnetization correlation function $F(t)$ of an $N \times N$ spin lattice.

The relaxation times for systems with $N=3,4,5$ show pronounced maxima at temperatures $T_m(N)$ near the critical temperature T_c of the infinite system. The systems investigated appear to be too small to reproduce the finite-size scaling behavior of $T_m(N)$ discussed for the specific heat by Fisher and Ferdinand⁴³ and by Fisher.⁴⁴

VI. SUMMARY

We applied the generalized moment expansion (GME), an approximation scheme for dynamical observables in stochastic systems, to finite (size N) Ising models.

First we considered the one-dimensional Glauber model with transition rates (2.3) for $\delta=0$. We demonstrated the quality of our expansion by comparing the [3,3] GME approximant to the spin autocorrelation function with an exact expression, i.e., (2.14). We then considered transition rates for arbitrary δ in the range $-1 < \delta < +1$. We identified a slow phase in the spin autocorrelation function for $\delta=-1$. In this limit dynamical processes become nonergodic.

For the magnetization correlation function we investigated the critical slowing down of the relaxation process near $T=0$. We found that the critical dynamical exponent z , known for the infinite system to assume the

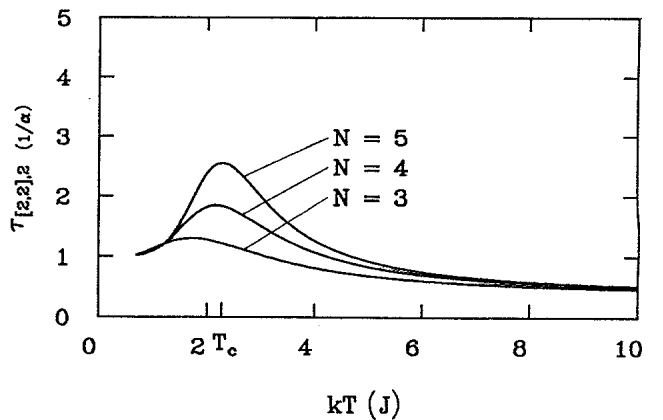


FIG. 11. Same as Fig. 10, but $\tau_{[2,2],2}$ instead of $\tau_{[2,2],1}$.

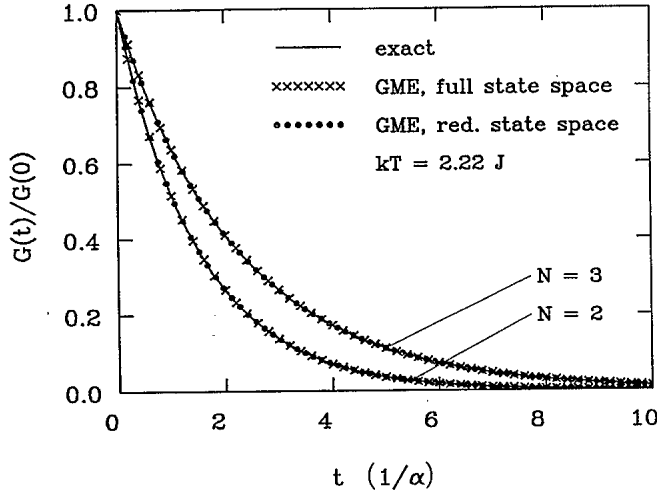


FIG. 12. Comparison between the magnetization intensity correlation function $G(t)$ for 2×2 and 3×3 spin lattices evaluated exactly and evaluated by means of [3,3] GME in reduced and full state space.

value 2 (Ref. 8), takes on the same value for finite systems rather independent of the size N . For a temperature-dependent δ as described by (4.11) we determined an exponent $z=4$. In the limit $\delta \rightarrow -1$ a temperature-dependent δ yields also the exponent $z=4$, which in this case arises from nonergodic behavior and appears only in finite systems.

In order to study nonexponential Williams-Watts behavior of correlation functions we suggested a modified expansion scheme based on the moments μ_0 , μ_{-1} , and μ_{-2} of the exact correlation function, which directly determines the Williams-Watts parameters a , τ , and β . For vanishing δ as well as for δ values not close to the boundary of the δ interval $[-1,1]$ the spin autocorrelation function was found to agree well with the Williams-

Watts form ($\beta \approx 0.7$, see Fig. 6). Close to the boundaries the relaxation process is characterized by nonergodic behavior with two very distinct relaxation times. The magnetization correlation function is found to be rather monoexponential, i.e., $\beta \approx 1$, for most values of δ .

The numerical effort required for the GME method restricts applications to systems with 16–25 spins, depending on computational resources. To extend this size limit we introduced a coarse graining of the state space by collecting spin configurations into subsets and neglecting the detailed distribution in these substates. Choosing subsets to collect all configurations with identical magnetization we reduced the dimension of the transition matrix from 2^N to $N+1$ and obtained accurate magnetization correlation functions for larger systems except near $\delta = +1$.

We finally applied the GME and the reduced state space approximation to two-dimensional Ising models. We determined magnetization (intensity) correlation functions and, thereby, reproduced critical slowing down in these systems.

In conclusion we like to remark on the possibilities to increase the dimension of master equations treated by the GME. Master equations are represented by sparse matrices. The computational effort of the GME is mainly determined by the number of nonvanishing matrix elements. The largest number of nonvanishing matrix elements treated in our examples on a minicomputer was 6×10^5 . The storage of today's supercomputers (large rapid access memory and solid state disks) allow one easily to increase this number by two orders of magnitude. Also, the processing units in recent supercomputers are well suited to solve rapidly the linear equations to obtain the generalized moments. We expect that the GME will be a valuable tool for the study of stochastic systems with critical behavior.

ACKNOWLEDGMENT

This work has been supported by the Deutsche Forschungsgemeinschaft (Schu 523).

APPENDIX: EXACT SOLUTION FOR THE SPIN AUTOCORRELATION FUNCTION IN A FINITE RING

Glauber's derivation of the spin autocorrelation function $\langle \sigma_k(t) \sigma_i(0) \rangle$ in the special case of vanishing δ can readily be generalized to finite rings of length N by modifying one step in the original derivation.³ We will use the same notation as Ref. 3 and start from Glauber's Eqs. (60) and (61). Since we want to impose periodic boundary conditions, we require $r_0(t)$ to be equivalent to $r_N(t)$. Equations (60) and (61) are then to be replaced by

$$\frac{d}{dt} r_m(t) = -2r_m(t) + \gamma[r_{m-1}(t) + r_{m+1}(t)] \quad (\text{A1})$$

for $m \neq 0$, and

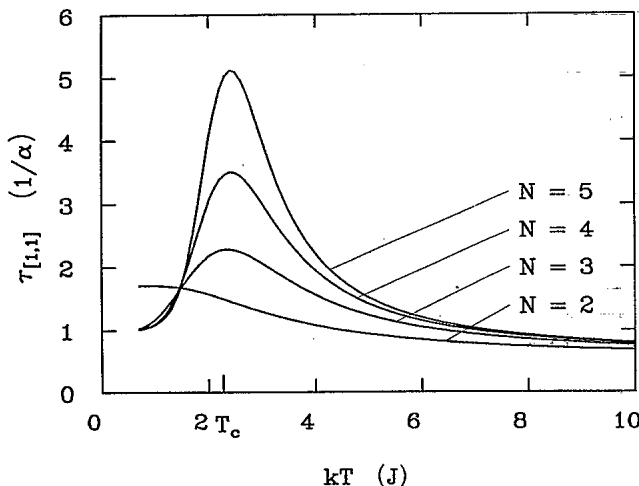


FIG. 13. Comparison of mean relaxation times $\tau_{[1,1]}$ of the magnetization intensity correlation function $G(t)$ for systems of different size; $G(t)$ has been evaluated in the reduced state space.

$$r_0(t) = r_N(t) = 1. \quad (\text{A2})$$

At equilibrium the left-hand side of Eq. (A1) vanishes. To solve the resulting equation we set

$$r_m = \frac{1}{1 + \eta^N} (\eta^m + \eta^{N-m}), \quad 0 \leq m \leq N. \quad (\text{A3})$$

This solution meets boundary condition (A2) and satisfies (A1) when η is chosen identical with Glauber's original η , namely,

$$\eta = \frac{1}{\gamma} [1 - (1 - \gamma^2)^{1/2}]. \quad (\text{A4})$$

For the correlation function $\langle \sigma_k(t) \sigma_j(0) \rangle$ in thermal

equilibrium Eq. (A3) leads to a modification of Glauber's Eq. (75)

$$\langle \sigma_k(t) \sigma_j(0) \rangle = e^{-\alpha t} \sum_{l=1}^N \sum_{i=-\infty}^{\infty} I_{k-l+iN}(\gamma \alpha t) \times \frac{\eta^{|j-l|} + \eta^{N-|j-l|}}{1 + \eta^N}. \quad (\text{A5})$$

In the limit $N \rightarrow \infty$ only the terms $i=0$ and $i=1$ contribute, and Glauber's results (75) is recovered

$$\langle \sigma_k(t) \sigma_j(0) \rangle = e^{-\alpha t} \sum_{l=-\infty}^{\infty} I_l(\gamma \alpha t) \eta^{|j-k+l|}. \quad (\text{A6})$$

*Present address: Arthur Amos Noyes Laboratory of Chemical Physics, California Institute of Technology, Pasadena, CA 91125.

¹S. G. Brush, *Rev. Mod. Phys.* **39**, 883 (1967).

²L. Onsager, *Phys. Rev.* **65**, 117 (1944).

³R. J. Glauber, *J. Math. Phys.* **4**, 294 (1963).

⁴B. U. Felderhof, *Rep. Math. Phys.* **1**, 215 (1971).

⁵A. Baumgärtner and K. Binder, *J. Stat. Phys.* **18**, 423 (1978).

⁶H. J. Hilhorst, *Physica A* **79**, 171 (1975).

⁷R. H. Lacombe, *J. Macromol. Sci. Phys. B* **18**, 697 (1980).

⁸Y. Achiam, *J. Phys. A* **11**, 975 (1978).

⁹U. Dekker and F. Haake, *Z. Phys. B* **35**, 281 (1979).

¹⁰J. C. Kimball, *J. Stat. Phys.* **21**, 289 (1979).

¹¹F. Haake and K. Thol, *Z. Phys. B* **40**, 219 (1980).

¹²W. Zwirger, *Phys. Lett.* **84A**, 269 (1981).

¹³R. Pandit, G. Forgacs, and P. Rujan, *Phys. Rev. B* **24**, 1576 (1981).

¹⁴M. Schwarz, Jr. and D. Poland, *J. Chem. Phys.* **56**, 2620 (1976).

¹⁵D. Poland and H. A. Scheraga, *Theory of Helix-Coil Transitions in Biopolymers* (Academic, London, 1970).

¹⁶J. E. Anderson, *J. Chem. Phys.* **52**, 2821 (1970).

¹⁷D. J. Isbister and D. A. McQuarrie, *J. Chem. Phys.* **60**, 1937 (1974).

¹⁸S. Bozdemir, *Phys. Status Solidi B* **103**, 459 (1981); **104**, 37 (1981).

¹⁹J. E. Shore and R. Zwanzig, *J. Chem. Phys.* **63**, 5445 (1975).

²⁰S. H. Glarum, *J. Chem. Phys.* **33**, 1371 (1960).

²¹G. D. Patterson, in *Advances in Polymer Sciences*, edited by J. D. Ferry (Springer, Berlin, 1983), Vol. 48, p. 125.

²²G. Williams and D. C. Watts, *Trans. Far. Soc.* **67**, 80 (1970).

²³G. Williams, D. C. Watts, S. B. Dev, and A. M. North, *Trans. Far. Soc.* **67**, 1323 (1971).

²⁴P. Bordewijk, *Chem. Phys. Lett.* **32**, 592 (1975).

²⁵M. F. Shlesinger and E. W. Montroll, *Proc. Natl. Acad. Sci. U.S.A.* **81**, 1280 (1984).

²⁶J. L. Skinner, *J. Chem. Phys.* **79**, 1955 (1983).

²⁷J. Budimir and J. L. Skinner, *J. Chem. Phys.* **82**, 5232 (1985).

²⁸K. Schulten, Z. Schulten, and A. Szabo, *J. Chem. Phys.* **74**, 4426 (1981).

²⁹K. Schulten, A. Brünger, W. Nadler, and Z. Schulten, in *Synergetics—From Microscopic to Macroscopic Order*, edited by E. Frehland (Springer, Berlin, 1984), p. 80.

³⁰A. Brünger, R. Peters, and K. Schulten, *J. Chem. Phys.* **82**, 2147 (1985).

³¹W. Nadler and K. Schulten, *Phys. Rev. Lett.* **51**, 1712 (1983).

³²W. Nadler and K. Schulten, *J. Chem. Phys.* **82**, 151 (1985).

³³W. Nadler and K. Schulten, *Z. Phys. B* **59**, 53 (1985).

³⁴W. Nadler and K. Schulten, *J. Chem. Phys.* **84**, 4015 (1986).

³⁵Such clustering requires appropriate β_n values.

³⁶M. N. Barber, in *Phase Transitions and Critical Phenomena*, edited by C. Domb and J. L. Lebowitz (Academic, London, 1983), Vol. 8, p. 146.

³⁷W. B. Jons, W. J. Thron, and H. Waadeland, *Trans. Am. Math. Soc.* **261**, 503 (1980).

³⁸A. Brünger, Ph.D. thesis, Technical University, Munich, 1982.

³⁹W. Nadler, Ph.D. thesis, Technical University, Munich, 1985.

⁴⁰This solution is a trivial generalization of that given in Ref. 32 and in K. Schulten, *Chem. Phys. Lett.* **124**, 230 (1986).

⁴¹D. R. Kincaid, J. R. Respass, D. M. Young, and R. G. Grimes, Itpack 2C: A FORTRAN Package for Solving Large Sparse Linear Systems by Adaptive Accelerated Iterative Methods, *ACM Transactions on Mathematical Software* **8**, 302 (1982).

⁴²E. Stoll, K. Binder, and T. Schneider, *Phys. Rev. B* **8**, 3266 (1973).

⁴³M. E. Fisher and A. E. Ferdinand, *Phys. Rev. Lett.* **19**, 169 (1967).

⁴⁴M. E. Fisher, in *Critical Phenomena, Proceedings of the 51st Enrico Fermi Summer School, Varenna, Italy, 1970*, edited by M. S. Green (Academic, New York, 1971).